Pergamon

Int. J. Solids Structures Vol. 35, No. 13, pp. 1339–1353, 1998

0020–7683/98 $19.00 + .00

PII: S0020–7683(97)00095–4

MODELING OF DOMAIN SWITCHING IN FERROELECTRIC CERAMICS: AN EXAMPLE

YONGZHONG HUO and QING JIANG†
Department of Engineering Mechanics, Center for Materials Research and Analysis, University of Nebraska-Lincoln, 212 Bancroft Hall, PO Box 880 347, Lincoln, Nebraska 68588-0347, U.S.A.

(*Received* 8 *February* 1996; *in revised form* 18 *March* 1997)

Abstract—The authors have recently proposed a continuum model for domain switching in polycrystalline ferroelectric ceramics in which each crystallite is modeled as a mixture of various domains characterized by their mass fractions, and domain switching corresponds to changes of the mass fractions of the corresponding domains. In order to explore the implications of this model, the authors present the explicit solution to an idealized one-dimensional ferroelectric system. The solution indicates that the orientation misalignment of crystallites results in a local electric field of strong inhomogeneity. The local electric field does not necessarily vanish in the absence of an externally applied electric field and its magnitude at certain locations can be substantially larger than that of the externally applied electric field. With a postulated domain switching criterion, the model produces the hysteretic response of the macroscopic polarization to the applied electric field due to local domain switching. © 1998 Elsevier Science Ltd.

1. INTRODUCTION

Ferroelectric crystals have been increasingly used to design actuators (Cross, 1993) for various applications, such as active control of large flexible space trusses (Crawley and de Luis, 1978), structural acoustics (Cross, 1994; Kim *et al.* 1996) and helicopter rotary blades (Samak and Chopra, 1993, 1994; Giurgiutiu *et al.* 1994). The major obstacle in these applications is the so-called electric fatigue which refers to deterioration of material properties (Salaneck, 1972; Carl, 1975). A number of experimental observations (Jiang and Cross, 1993; Jiang *et al.*, 1994; Park and Sun, 1995; Freiman and White, 1995; White *et al.*, 1996; Hill *et al.*, 1996; Lynch, 1996) indicate that fatigued specimens often contain microcracks, i.e., cracks of length comparable to the grain size which is typically 5 μm in average. The cause of microcracking is generally attributed to stress and electric field concentrations at the grain level due to material inhomogeneity although the detailed mechanism is still under investigation (Suo *et al.*, 1992; Cao and Evans, 1994; Jiang, 1994; Zhang and Jiang, 1995). Development of continuum models remains a challenging task because of the evolving microstructure and the polycrystalline nature of these materials.

The commonly-used ferroelectric materials in actuator applications are the polycrystalline oxide ceramics of barium titanate ($BaTiO_3$) and PZT ($Pb[Zr, Ti]O_3$). Barium titanate and PZT both have the perovskite cubic structure in the paraelectric phase. At room temperature, barium titanate has a tetragonal structure. While PZT has a tetragonal structure on the Ti-rich side and has a rhombohedral structure on the Zr-rich side except on the extreme Zr-rich side where the solid solution exhibits no observable ferroelectric effect. The commonly-used PZT is on the Ti-rich side near its morphotropic phase boundary because of the strong electromechanical coupling effect. The tetragonal structure is polar in the sense that the centers of positive and negative charges for each lattice unit are spatially separated, forming a dipole of electric charges. Consequently, these crystals exhibit spontaneous polarization. In a stable configuration, each crystallite is divided into a number of macroscopic regions in which the polar directions differ from each other by either 180° or approximately 90°. The deviation from 90° is determined by the lattice parameters. These

† Author to whom correspondence should be addressed.

regions are called the *ferroelectric domains* and correspondingly, the interfaces are referred to as the 180° or 90° *domain walls*, respectively.

The commercial barium titanate and PZT ceramics are produced as polycrystalline solid solutions through the conventional steps of sintering of fine powders of oxide metals. The resulting solid solutions do not exhibit observable electromechanical coupling effect because the ferroelectric domains are so formed that the average polarization of each grain is approximately zero. Application of an electric field can switch the polar direction of a domain by either 180° or approximately 90°, called 180° or 90° *domain (polarization) switching*, respectively, and the resulting polar direction is closer to the direction of the applied electric field. The ceramics exhibit the electromechanical coupling effect only after the domains are reoriented by application of a strong DC field. This reorientation process is the so-called *poling process*. Ferroelectric domains are initially formed when the ceramics are cooled from high processing temperatures and they are altered during the subsequent poling process, leading to a macroscopic polarization, called the *remnant polarization*. Application of an electric field can change the remnant polarization, both its magnitude and direction, resulting in a macroscopic displacement, or a force when the ceramic is clamped. This provides the mechanism of electrically-controlled actuation (Cross, 1993).

Kim and Jiang (1996) proposed a continuum model to simulate the microcracking effect on macroscopic properties of polycrystalline ferroelectric ceramics. Their predictions on the microcracking-induced evolution of the electric field-polarization response and the resulting reduction of the remnant polarization are in qualitative agreement with the experimental observations. In their model, Kim and Jiang (1996) treat each grain as an effective domain by taking the average of the polarization intensities of the domains within the grain to be the effective polarization. Due to lack of a mechanism to determine the magnitude of the effective polarization intensity, they had to assign it a value rather arbitrarily in their numerical simulations. As a continuing effort to model domain switching in polycrystalline ferroelectric ceramics, we (Huo and Jiang, 1996) have recently proposed to model each grain as a body of mixture consisting of distinct types of domains which are characterized by their mass fractions as internal variables. Consequently, the average polarization of a grain is a linear function of the mass fractions and domain switching corresponds to changes of mass fractions of the corresponding domains. Because of its complications, any attempt to simulate a realistic system with this model would require a massive amount of computational work. In order to explore the implications of this model, we have studied an idealized one-dimensional system, and the detailed analysis is presented in this article. In the next section, we present our idealization of a ferroelectric specimen to a ferroelectric plate consisting of N layers of crystallites with distinct orientations. Neglecting the edge effect, we assume that each of the variables varies only along the plate thickness direction and this leads to a one-dimensional system. Thanks to the simple setting, we have obtained the solution in an explicit form which allows us to study the implications of our model on the inhomogeneous distribution of the local electric field. In the one-dimensional framework, the law of mechanical equilibrium requires that the axial stress remains constant spatially. This prevents us from studying the polycrystalline effect on stress distributions, i.e., stress concentrations at the grain level. We thus focus the present analysis on distributions of local electric field. We devote Section 3 to a study of the implications of the second law of thermodynamics on this idealized system. We show that equilibrium requires minimization of a potential energy which leads to the determination of the mass fractions of distinct domains in all the crystallites. There are two groups of minimizers, distinguished by whether or not some of the crystallites are saturated in polarization. We then turn to study quasi-static processes in Section 4. As expected, there is no hysteresis in the dielectric response to the applied electric field in any quasi-static process in which only minimizers are accessible. Our previous analysis (Huo and Jiang, 1996), based on thermodynamics, indicates that the driving force for domain switching in this model is the difference of the Gibbs free energies associated with the corresponding domains. To model the hysteretic response of macroscopic polarization to applied electric field due to domain switching within grains, we postulate that there exists a material property, called the critical driving force and that domain switching takes place whenever

the driving force exceeds this critical value. The resulting numerical results, presented in Section 5, indicate that mismatch of polarization among crystallites results in an inhomogeneous electric field whose magnitude at certain locations can be substantially larger than that of externally applied electric field, and that the internal electric field does not necessarily vanish in the absence of externally applied electric field.

We note that ferroelectric domains are, from the kinematics point of view, analogous to twin plates associated with martensitic phase transformations. Owing to the pioneering work of Ericksen (1975), Knowles and Sternberg (1975), Abeyaratne (1980), James (1981) and others, continuum modeling of solid-solid phase transitions has become a very active area of research in mechanics and materials. The investigations in this area closely related to the present work are the work of Ball and James (1987) on the fine phase mixtures in martensitic phase transformations, the work of Abeyaratne and Knowles (1988) on the kinetics of phase boundaries, and the recent work of James and Kinderlehrer (1993) on the domain structures in ferromagnetic materials.

2. AN IDEALIZED ONE-DIMENSIONAL SYSTEM

Many specimen for fatigue test are of a plate-like geometry. The upper and lower surfaces are electroded so that an electric field can be applied across its thickness. In order to render a one-dimensional model, we consider such a plate being composed of N layers of crystallites with thickness h_n, $n = 1, 2, \ldots, N$. Let the x-axis be along the thickness direction with the nth layer occupying the interval $[x_n, x_{n+1}]$. The orientation of the nth crystallite is characterized by the orientation tensor $\mathbf{R}_n$. Let us consider the case that the paraelectric-to-ferroelectric phase transformation corresponds to a cubic-to-tetragonal transformation in the crystal lattice structure, and hence each of these crystallites consists of six distinct types of domains whose polar directions are mutually orthogonal. Their spontaneous polarization intensities admit the following representations:

$$\mathbf{p}_\alpha^s(n) = p^s \mathbf{R}_n \mathbf{Q}_\alpha \mathbf{E}_x^0, \quad \alpha = 1, 2, \ldots, 6; \quad n = 1, 2, \ldots, N. \tag{1}$$

Here, p^s denotes the spontaneous polarization magnitude and $\mathbf{E}_x^0$ the unit vector along the x-direction. $\mathbf{Q}_\alpha$, $\alpha = 1, 2, \ldots, 6$, are the six orthogonal tensors that form the point group of the crystal cubic lattice. The matrix representations of these orthogonal tensors in the lattice frame are given by

$$\mathbf{Q}_1 = -\mathbf{Q}_2 = \begin{pmatrix} 1 & 0 & 0 \\ 0 & 1 & 0 \\ 0 & 0 & 1 \end{pmatrix}, \quad \mathbf{Q}_3 = -\mathbf{Q}_4 = \begin{pmatrix} 0 & -1 & 0 \\ 1 & 0 & 0 \\ 0 & 0 & 1 \end{pmatrix}, \quad \mathbf{Q}_5 = -\mathbf{Q}_6 = \begin{pmatrix} 0 & 0 & -1 \\ 0 & 1 & 0 \\ 1 & 0 & 0 \end{pmatrix}. \tag{2}$$

We define the macroscopic spontaneous polarization (Huo and Jiang, 1996) of the nth crystallite as the following average:

$$\mathbf{p}_n^s(\mathbf{z}^n) = \sum_{\alpha=1}^{6} z_\alpha^n \mathbf{p}_\alpha^s(n), \quad n = 1, 2, \ldots, N, \tag{3}$$

where z_α^n, $\alpha = 1, 2, \ldots, 6$, denote the mass fractions of the six distinct types of domains within the nth crystallite and they satisfy the following constraints:

$$z_\alpha^n \geqslant 0, \quad \alpha = 1, 2, \ldots, 6; \quad \text{and} \quad \sum_{\alpha=1}^{6} z_\alpha^n = 1, \quad n = 1, 2, \ldots, N. \tag{4}$$

Let us first consider an electro-mechanical static process. The Faraday's law requires that

the electric field intensity **e** be curl-free within each of the crystallites, and hence there exists a continuous and piecewise differentiable function ϕ, called the electric voltage potential, such that

$$\mathbf{e} = -\nabla\phi \quad \text{within every crystallite.} \tag{5}$$

We consider the case that the voltages at both the upper and the lower surfaces of the specimen are specified, and this corresponds to the following boundary conditions

$$\phi = 0 \quad \text{at} \quad x = 0; \quad \phi = V \quad \text{at} \quad x = H, \tag{6}$$

where H denotes the thickness of the plate and V the voltage drop, related to the applied electric field e_a through $e_a = -V/H$. Neglecting the edge effect, we assume that the electrical voltage potential depends only upon the coordinate x, and consequently, the electric field is along the thickness direction. To render a one-dimensional problem, we assume, rather arbitrarily, that the stress tensor has only one non-zero component, i.e., the normal stress along the thickness. In the absence of body forces, equilibrium requires that the stress remains constant throughout the specimen.† We take it as zero because usually no mechanical loads are applied in electric fatigue tests. In the absence of stresses, the macroscopic polarization **p** is related to the macroscopic electric field intensity **e** through the following constitutive relation

$$\mathbf{p} = \mathbf{p}_n^s(\mathbf{z}^n) + \mathscr{Y}^n(\mathbf{z}^n)\mathbf{e}, \quad \text{within the } n\text{th crystallite} \tag{7}$$

where the dielectric susceptibility tensor (Huo and Jiang, 1996) of the nth crystallite is given as

$$\mathscr{Y}^n(\mathbf{z}^n) = \sum_{\alpha=1}^{6} z_\alpha^n \mathbf{R}_n \mathbf{Q}_\alpha \mathscr{Y}_0 \mathbf{Q}_\alpha^{\mathrm{T}} \mathbf{R}_n^T, \quad n = 1, 2, \ldots, N. \tag{8}$$

Here, $\mathscr{Y}_0$ stands for the dielectric susceptibility tensor of the single-domain crystal in the tetragonal phase and its matrix representation in the lattice frame has the diagonal form

$$\mathscr{Y}_0 = \begin{pmatrix} \eta_c & 0 & 0 \\ 0 & \eta_a & 0 \\ 0 & 0 & \eta_a \end{pmatrix}, \tag{9}$$

with η_a and η_c being the dielectric susceptibility constants along the tetragonal a-axis and the tetragonal c-axis, respectively. It is implied by (7) that the polarization intensity **p** varies only with one coordinate, x, and so does the dielectric displacement **d**, defined as $\mathbf{d} = \mathbf{e} + \mathbf{p}$. Coulomb's law requires that the x-component of **d**, in the absence of free charges, remain constant throughout the specimen, and we denote it by d. From the constitutive relation (7), we obtain

$$d = p_n^s(\mathbf{z}^n) + \varepsilon_n(\mathbf{z}^n)e(x), \quad x_{n-1} \leqslant x \leqslant x_n, \quad n = 1, 2, \ldots, N, \tag{10}$$

where $p_n^s(\mathbf{z}^n)$ stands for the x-component of the macroscopic spontaneous polarization of the nth crystallite and e the magnitude of the electric field intensity. The dielectric permittivity along the thickness $\varepsilon_n(\mathbf{z}^n)$ for the nth crystallite is related to the corresponding dielectric susceptibility tensor $\mathscr{Y}^n(\mathbf{z}^n)$ through $\varepsilon_n(\mathbf{z}^n) = 1 + [\mathscr{Y}^n(\mathbf{z}^n)\mathbf{E}_x^0] \cdot \mathbf{E}_x^0$, with $\mathbf{E}_x^0$ being the unit vector along the x direction. The modified constitutive relation (10) implies that the

† As pointed out by one of the reviewers, the one-dimensional setting has essentially simplified the polycrystalline body to an array of single crystal aggregates and it has prevented us from studying the mechanical interactions among grains of distinct orientation.

electric field e remains constant within each of the crystallites. We denote its value within the nth crystallite by e_n and we turn now to determine its value within each of the crystallites. Integrating eqn (5) with the boundary condition (6) yields

$$\sum_{n=1}^{N} h_n e_n = H e_a. \tag{11}$$

This relation together with (10) leads to the electric field within each of the crystallites as follows:

$$e_n = e_n(\{\mathbf{z}^n\}_{n=1}^N, e_a) = \frac{d - p_n^s}{\varepsilon_n}, \quad n = 1, 2, \ldots, N, \tag{12}$$

where

$$d = d(\{\mathbf{z}^n\}_{n=1}^N, e_a) = \frac{H e_a + \sum_{m=1}^{N} h_m p_m^s / \varepsilon_m}{\sum_{m=1}^{N} h_m / \varepsilon_m}. \tag{13}$$

As indicated above, the dielectric displacement d depends on the mass fractions of distinct domains of all the crystallites, and so does the electric field within every crystallite because of the relations (12). In the next section, we turn to the determination of these mass fractions.

3. IMPLICATIONS OF THE DISSIPATION INEQUALITY

3.1. *The dissipation inequality*

In the current one-dimensional setting where stresses vanish identically and the absolute temperature θ remains constant, the second law of thermodynamics leads to the following dissipation inequality (Huo and Jiang, 1996):

$$\rho\theta\gamma_n = -\rho\dot{g}_n - p_n\dot{e}_n \geqslant 0, \quad n = 1, 2, \ldots, N, \tag{14}$$

where γ_n stands for the entropy production of the nth crystallite, and ρ the mass density assumed to be constant. The Gibbs free energy density g_n of the nth crystallite is defined by

$$g_n = \sum_{\beta=1}^{6} z_\beta^n g_\beta^n, \quad n = 1, 2, \ldots, N, \tag{15}$$

where the Gibbs free energy density g_β^n associated with the β-domain of the nth crystallite is given (Huo and Jiang, 1996) as follows:

$$\rho g_\beta^n = \rho f_0 - \tfrac{1}{2}\eta_\beta^n e_n^2 - e_n p_\beta^s(n), \quad \beta = 1, 2, \ldots, 6, \quad n = 1, 2, \ldots, N. \tag{16}$$

Here, the constant f_0 denotes the Helmholtz free energy density associated with the β-domain, at the temperature θ and in the absence of both stresses and electric fields. We denote, respectively, by η_β^n and $p_\beta^s(n)$, the corresponding susceptibility coefficient along the x direction and the x-component of the corresponding spontaneous polarization, i.e.

$$\eta_\beta^n = (\mathscr{Y}_\beta^n \mathbf{E}_x^0) \cdot \mathbf{E}_x^0, \quad p_\beta^s(n) = p_0^s(\mathbf{R}_n \mathbf{Q}_\alpha \mathbf{E}_x^0) \cdot \mathbf{E}_x^0, \quad \beta = 1, 2, \ldots, 6, \quad n = 1, 2, \ldots, N. \tag{17}$$

Summing (14) over all the crystallites leads to the total entropy production

$$\Gamma = \sum_{n=1}^{N} \rho h_n \gamma_n = -\frac{1}{\theta}\frac{\mathrm{d}}{\mathrm{d}t}(G_e(\{\mathbf{z}^n\}_{n=1}^N; \quad e_a) + He_a d) \geqslant 0, \tag{18}$$

where the potential energy G_e is defined as

$$G_e(\{\mathbf{z}^n\}_{n=1}^N; \quad e_a) = \sum_{m=1}^{N} h_m \left(\sum_{\beta=1}^{6} \rho z_\beta^m g_\beta^m - \frac{1}{2} e_m^2 \right). \tag{19}$$

In arriving at (18), we have used relation (11) and the fact that the dielectric displacement d remains constant. The dissipation inequality (18) suggests that the potential energy $G_e(\{\mathbf{z}^n\}_{n=1}^N; \quad e_a)$ should attain its minimum at equilibrium when the applied electric field is kept constant. Noting that the mass fractions must satisfy the constraints (4), one should minimize the functional

$$\Psi(\{z_\alpha^n\}_{\alpha,n}, \{\lambda_n\}_n) = G_e - \sum_{m=1}^{N} \lambda_m \left(\sum_{\beta=1}^{6} z_\beta^m - 1 \right), \tag{20}$$

where λ_m are the Lagrangian multipliers.

The constraints in (4) confine all the minimizers of the potential energy $G_a(\cdot; e_a)$ in the super-cubic region $\mathscr{R} \equiv \{\{\mathbf{z}^n\}_{n=1}^N; \quad 0 \leqslant z_\alpha^n \leqslant 1\}$ of the $6N$-dimensional space. There are two distinct cases: (i) a minimizer is an interior point of $\mathscr{R}$; and (ii) a minimizer is on the boundary of $\mathscr{R}$. In the latter case, there is at least one crystallite for which one of the mass fractions is equal to 1 and the rest are all equal to zero, and we refer to it as a saturated minimizer because it indicates that the crystallite has reached a state of saturation of polarization. A minimizer within the interior of $\mathscr{R}$ is called an interior minimizer. The following two subsections are devoted to the discussion of these two distinct cases, respectively.

3.2. *Interior minimizers*

At an interior minimizer, we should have from (20)

$$\frac{\partial G_e}{\partial z_\alpha^n} - \lambda_n = 0, \quad \alpha = 1, 2, \ldots, 6, \quad n = 1, 2, \ldots, N. \tag{21}$$

Differentiating (19) with respect to the mass fraction z_α^n and invoking (16) yield

$$\frac{\partial G_e}{\partial z_\alpha^n} = h_n \rho g_\alpha^n - \sum_{m=1}^{N} h_m (p_m^{\vee}(\mathbf{z}^m) + (1 + \eta_m(\mathbf{z}^m)) e_m) \frac{\partial e_m}{\partial z_\alpha^n} \tag{22}$$

Substituting (11) and (12) into the above and noting that the applied electric field e_a is kept constant, we obtain

$$\frac{\partial G_e}{\partial z_\alpha^n} = h_n \rho g_\alpha^n, \quad \alpha = 1, 2, \ldots, 6, \quad n = 1, 2, \ldots, N. \tag{23}$$

Therefore from (21), at an interior minimizer, the six types of domains within the same crystallite must all have equal Gibbs free energy densities, i.e.

$$g_\alpha^n = g_\beta^n \quad \alpha, \beta = 1, 2, \ldots, 6, \quad n = 1, 2, \ldots, N. \tag{24}$$

From (16) we have

$$\rho(g_\alpha^n - g_\beta^n) = -\tfrac{1}{2}(\eta_\alpha^n - \eta_\beta^n)e_n^2 - (p_\alpha^s(n) - p_\beta^s(n))e_n, \quad \alpha,\beta = 1,2,\ldots,6, \quad n = 1,2,\ldots,N. \tag{25}$$

Since the polar directions of the six distinct types of domains within the same crystallite are mutually orthogonal, there are always two types of domains whose polar directions are opposite and whose spontaneous polarization intensities have non-zero x-components. For such a pair of domain types, the x-components of their spontaneous polarization intensities are equal in magnitude but of opposite signs, and their susceptibility coefficients along the x-direction are equal, i.e.

$$p_{\delta^+(n)}^s(n) = -p_{\delta^-(n)}^s(n) \quad \text{and} \quad \eta_{\delta^+(n)}^n = \eta_{\delta^-(n)}^n, \quad n = 1,2,\ldots,N. \tag{26}$$

where $\delta^+(n)$ and $\delta^-(n)$ are designated to such a domain pair for the nth crystallite. For the convenience of later discussion, the $\delta^+(n)$-domain is identified as the type of domain with the nth crystallite whose x-component of the spontaneous polarization is the largest. Consequently, the $\delta^-(n)$-domain is the type of domain within the nth crystallite whose x-component of the spontaneous polarization is the smallest. Recalling (3), the definition of the macroscopic spontaneous polarization, one sees that $p_{\delta^+(n)}^s(n)$ and $p_{\delta^-(n)}^s(n)$ are, respectively, the maximum and the minimum of the spontaneous polarization along the x-direction for the nth crystallite. Letting $\sigma = \delta^+(n)$ and $\beta = \delta^-(n)$ in (25) and invoking equalities (24) and (26), we conclude that the electric field vanishes identically within each of the crystallites, i.e.

$$e_n = 0, \quad n = 1,2,\ldots,N. \tag{27}$$

Hence, an interior minimizer can be attained only in the absence of applied electric field, i.e., $e_a = 0$. Correspondingly, from (7) and (12) we have

$$p_n(\mathbf{z}^n) = p_n^s(\mathbf{z}^n) = d, \quad n = 1,2,\ldots,N, \tag{28}$$

i.e., the polarizations along the x-direction are the same for all the crystallites and they are equal to the macroscopic dielectric displacement d which may not necessarily be zero although the applied electric field has to be zero at interior minimizers. To determine the possible values of d, we recall the designations of $\delta^+(n)$ and $\delta^-(n)$, i.e.

$$p_{\delta^-(n)}^s(n) \leqslant p_\alpha^s(n) \leqslant p_{\delta^+(n)}^s(n), \quad \alpha = 1,2,\cdot,6, \quad n = 1,2,\ldots,N. \tag{29}$$

Multiplying (29) by z_α^n and then summing the resulting over all the six types of domains for each of the crystallites yield

$$p_{\delta^-(n)}^s(n) \leqslant d = p_n^s(\mathbf{z}^n) \leqslant p_{\delta^+(n)}^s(n), \quad n = 1,2,\ldots,N. \tag{30}$$

This further leads to

$$p_{\delta^-(m_0)}^s(m_0) \leqslant d \leqslant p_{\delta^+(m_0)}^s(m_0) \tag{31}$$

where the number m_0 is designated to the crystallite whose maximal x-component of the spontaneous polarization is the smallest among all the crystallites, i.e.

$$p^s_{\delta^+(n)}(n) \geqslant p^s_{\delta^+(m_0)}(m_0), \quad n = 1, 2, \ldots, N. \tag{32}$$

3.3. *Saturated minimizers*

The above discussion indicates that there are no interior minimizers in the presence of an applied electric field. In this case, the local electric field should no longer vanish identically. We first consider the case that the local electric field vanishes in all the crystallites except one, the n_0th crystallite say, i.e.

$$e_{n_0} \neq 0 \quad \text{and} \quad e_n = 0, \quad \text{for } n \neq n_0. \tag{33}$$

From (11) and (10) we obtain

$$e_{n_0} = \frac{He_a}{h_{n_0}} \quad \text{and} \quad p_n = p^s_n = d, \quad \text{for } n \neq n_0. \tag{34}$$

For definiteness, we assume that e_a is positive, and consequently e_{n_0} is positive as well. The relation (25) indicates that for a sufficiently small e_a

$$g^{n_0}_{\delta^+(n_0)}(e_{n_0}) < g^{n_0}_{\alpha}(e_{n_0}), \quad \alpha \neq \delta^+(n_0). \tag{35}$$

In arriving the above, we have assumed that each crystallite has only one type of domains, designated as the $\delta^+(n)$-domains, whose x-component of spontaneous polarization is larger than those of the other types of domains.† Minimization of the Gibbs energy for the n_0th crystallite requires that

$$z^{n_0}_{\delta^+(n_0)} = 1, \quad \text{and} \quad z^{n_0}_{\alpha} = 0, \quad \textit{for } \alpha \neq \delta^+(n_0). \tag{36}$$

By (3) and (8) this implies that

$$p^s_{n_0} = p^s_{\delta^+(n_0)}(n_0) \quad \text{and} \quad \eta_{n_0} = \eta^{n_0}_{\delta^+(n_0)}, \tag{37}$$

that is, the spontaneous polarization $p^s_{n_0}$ of the n_0th crystallite reaches its maximum $p^s_{\delta^+(n_0)}(n_0)$, becoming saturated.

Substituting (34) and (37) into (10) yields

$$d = p^s_{\delta^-(n_0)}(n_0) + \varepsilon^{n_0}_{\delta^+(n_0)} \frac{He_a}{h_{n_0}}. \tag{38}$$

From (29), (3) and (34) we obtain

$$p^s_{\delta^+(n)}(n) \geqslant p^s_n = d > p^s_{\delta^+(n_0)}(n_0), \quad n \neq n_0. \tag{39}$$

Recalling (32), we concludes that the m_0th crystallite should first become saturated. Substituting (38) into the above and rearranging the resulting inequalities lead to the following upper bound for the applied electric field:

$$e_a \leqslant \frac{h_{m_0}}{H\varepsilon^{m_0}_{\delta^+(m_0)}}(p^s_{\delta^+(n)}(n) - p^s_{\delta^+(m_0)}(m_0)), \quad n \neq m_0. \tag{40}$$

Thus, as the applied electric field e_a increases and exceeds this upper bound, another

† In the case that a crystallite has two types of domains whose x-components of spontaneous polarization are both the largest, the discussion can be proceeded in a similar manner but the presentation is much more complicated.

crystallite would become saturated and it must be the one whose maximal x-component of the spontaneous polarization is the second smallest among all the crystallites. Furthermore, one can conclude that, as the applied electric field gets stronger, more crystallites would become saturated in the order of decreasing maximal x-component of the spontaneous polarization. For the convenience of our presentation, we renumber the crystallites in the order of decreasing maximal x-component of the spontaneous polarization, i.e.

$$p^s_{\delta^+(n)}(n) < p^s_{\delta^+(n+1)}(n+1), \quad n = 1, 2, \ldots, N-1. \tag{41}$$

This leads to the following construction of the saturated minimizers. In the case that the first k crystallites are saturated, one has

$$\begin{aligned} &e_n \neq 0, \quad p^s_n = p^s_{\delta^+(n)}(n), \quad \text{for } 1 \leqslant n \leqslant k, \\ &e_n = 0, \quad p_n = p^s_n = d \quad \text{for } k < n \leqslant N. \end{aligned} \tag{42}$$

Using (10) and (11) we obtain

$$d = \frac{He_a + \sum_{m=1}^{k} h_m p^s_{\delta^+(m)}(m)/\varepsilon^m_{\delta^+(m)}}{\sum_{m=1}^{k} h_m/\varepsilon^m_{\delta^+(m)}}, \tag{43}$$

and

$$e_n = \frac{d - p^s_{\delta^+(n)}(n)}{\varepsilon^n_{\delta^+(n)}}, \quad n \leqslant k. \tag{44}$$

By the same discussions as that lead to (39), and noticing (41), we should have the following inequalities:

$$p^s_{\delta^+(k+1)}(k+1) \geqslant d > p^s_{\delta^+(k)}(k). \tag{45}$$

substituting (43) into the above leads to the upper and lower bounds for the applied electric field e_a, i.e.

$$\sum_{m \leqslant k} \frac{h_m}{H\varepsilon^m_{\delta^+(m)}} (p^s_{\delta^+(k+1)}(k+1) - p^s_{\delta^+(m)}(m)) \geqslant e_a > \sum_{m \leqslant k-1} \frac{h_m}{H\varepsilon^m_{\delta^+(m)}} (p^s_{\delta^+(k)}(k) - p^s_{\delta^+(m)}(m)) \tag{46}$$

except in the case that $k = N$, indicating that all the crystallites have become saturated when the applied electric field becomes sufficiently strong. We then have a lower bound

$$e_a > \sum_{m=1}^{N-1} \frac{h_m}{H\varepsilon^m_{\delta^+(m)}} (p^s_{\delta^+(N)}(N) - p^s_{\delta^+(m)}(m)). \tag{47}$$

4. A DOMAIN SWITCHING CRITERION

We turn now to consider quasi-static processes in which the mass fractions vary with time in response to changes of applied electric field. It is evident that there is no hysteresis in the dielectric displacement response to the applied electric field for any quasi-static process in which only the minimizers are accessible. It is well known that the hysteretic behavior is one of the characteristics of ferroelectric materials (Jona and Shirane, 1962;

Jaffe *et al.*, 1971). This suggests that the specimen does not always attain the minimizers when domain switching takes place. Our previous work (Huo and Jiang, 1996) indicates that the driving force for switching α-domain to β-domain is the excess of the Gibbs energy associated with the α-domain over that associated with the β-domain, i.e., $g^n_\alpha - g^n_\beta$ for the nth crystallite. It is common (Abeyaratne and Knowles, 1988; Jiang, 1993; Tsai and Rosakis, 1995) to model hysteresis by introducing a threshold for the driving force and postulating that domain switching takes place only when the driving force exceeds this threshold. One may propose a rule that governs the rate of domain switching. Consequently, different rules would result in distinct hysteretic responses. For simplicity of this one-dimensional analysis, we postulate that when a driving force exceeds its threshold, the corresponding domain switching takes place, minimizing all the driving forces, i.e.

$$\Delta z^n_{\alpha\beta} = \begin{cases} >0, & \text{if } g^n_\alpha - g^n_\beta > \gamma^n_{\alpha\beta}, \\ <0, & \text{if } g^n_\alpha - g^n_\beta < -\gamma^n_{\alpha\beta},, \alpha,\beta = 1,2,\ldots,6, \\ =0, & \text{otherwise,} \end{cases}$$

$$\{\Delta z^n_{\alpha\beta}\}^6_{\alpha,\beta=1} \text{ minimizes } \sum_{\alpha,\beta=1}^{6} |g^n_\alpha - g^n_\beta|, \tag{48}$$

where $\Delta z^n_{\alpha\beta}$ denote the amount of materials in the nth crystallite being switched from the α-domain to the β-domain and $\gamma^n_{\alpha\beta}$, being positive, stands for the threshold of the corresponding driving force.

5. SOME NUMERICAL RESULTS

We now present some numerical results to illustrate the predictions of this model. The local constitutive relation contains three material parameters, i.e., the spontaneous polarization magnitude p^s, the dielectric susceptibility constants η_a and η_c, along the tetragonal a-axis and the tetragonal c-axis, respectively. Their values for $BaTiO_3$ at room temperature (Jona and Shirane, 1962) are given as follows:

$$p^s = 26 \times 10^{-6} \text{C/cm}^2, \quad \eta_a = 4099\varepsilon_0, \quad \eta_c = 159\varepsilon_o \tag{49}$$

where $\varepsilon_0 = 8.854 \times 10^{-12} \text{C}^2/\text{J} \cdot \text{m}$ is the permittivity of the vacuum. To model domain switching, we must specify the driving force threshold $\gamma^n_{\alpha\beta}$ for each of the crystallites. For simplicity, we assume that it has a constant value

$$\gamma^n_{\alpha\beta} \equiv 2p^s e_c, \tag{50}$$

where e_c is the so-called coercive field, i.e., the nominal strength of applied electric field required to initiate domain switching, often adopted by crystal physicists (Jona and Shirane, 1962), and its typical value for barium titanate is about 1.0 kV/cm.

We now specify the orientations of the crystallites. As discussed previously, each crystallite consists of six distinct types of domains whose polar directions are determined by the orientation of the unit in the cubic lattice which the crystal possesses at temperatures above the Curie point. Hence, we first specify the orientation of the cubic unit. For simplicity, we assume that all the crystallites have two of their principal axes of the cubic lattice in the same plane that contains the x axis. We refer to this plane as the $x-y$ plane and let the z axis perpendicular to this plane, forming a Cartesian frame X. Thus, one can determine the orientation of the cubic unit by specifying one of the principal axes within the $x-y$ plane, and this leads to the following matrix representation of the orientation tensor in the X frame:

$$\mathbf{R}_n = \begin{pmatrix} \cos\omega_n & -\sin\omega_n & 0 \\ \sin\omega_n & \cos\omega_n & 0 \\ 0 & 0 & 1 \end{pmatrix}. \tag{51}$$

where ω denotes the smaller angle among those that the two principal axes form with the x axis. Among the six distinct types of domains, two have their polar directions perpendicular to the $x-y$ plane, identified as Type 5 and Type 6, respectively, and the rest have their polar directions within the $x-y$ plane, identified as follows:

$$\omega_n^1 = \omega_n, \quad \omega_n^2 = \omega_n + \pi, \quad \omega_n^3 = \omega_n + \frac{\pi}{2}, \quad \omega_n^4 = \omega_n + \frac{3\pi}{2}. \tag{52}$$

Correspondingly, the x-components of the spontaneous polarization intensities and the susceptibility coefficients along the x direction are given as

$$P_\alpha^s(n) = p^s \cos\omega_n^\alpha, \quad \eta_\alpha^n = \eta_c \cos^2\omega_n^\alpha + \eta_a \sin^2\omega_n^\alpha, \quad \alpha = 1,2,3,4. \tag{53}$$

This leads to the maximum and the minimum of the macroscopic spontaneous polarization

$$p^s_{\delta^+(n)}(n) = p^s \cos\omega_n, \quad p^s_{\delta^-(n)}(n) = -p^s \cos\omega_n, \tag{54}$$

that is, $\delta^+(n) = 1$ and $\delta^-(n) = 2$. Noting that Type 5 and Type 6 should diminish upon application of an electric field parallel to the x axis, sufficiently strong to switch these domains, we exclude them from the following discussion by assuming that at the initial configuration

$$z_1^n = z_2^n = z_3^n = z_4^n = \tfrac{1}{4}, \quad z_5^n = z_6^n = 0, \quad n = 1,2,\ldots,N. \tag{55}$$

The orientation angle ω_n is within the range: $-\pi/4 < \omega_n < \pi/4$. From (53), one sees that two crystallites whose orientation angles are of equal magnitude but opposite sign should have the same constitutive behavior in this one-dimensional setting. We shall not distinguish them by restricting ω within the range: $0 \leqslant \omega_n < \pi/4$. A uniform partition of this range leads to

$$\omega_n = \left(1 - \frac{n}{N+1}\right)\frac{\pi}{4}, \quad n = 1,2,\ldots,N. \tag{56}$$

We now specify h_n, the thickness of the crystallites with orientation angle ω_n. We assume that all the orientations are of an equal preference. Thus orientation angle ω has a uniform distribution in the present simplified configuration due to the assumption that all the crystallites have two of their principal axes of the cubic lattice in the $x-y$ plane. If all the orientations in the three-dimensional space are considered to be of an equal preference, the orientation angle should have a spherical distribution, i.e., $h_n = C\sin\omega_n$, with C being a normalization constant. Noting that H stands for the thickness of the specimen, we obtain

$$h_n = \frac{4\left(1 - \cos\dfrac{\pi}{4(N+1)}\right)H\sin\omega_n}{(2-\sqrt{2})\sin\dfrac{\pi}{4(N+1)} - \sqrt{2}\left(1 - \cos\dfrac{\pi}{4(N+1)}\right)}, \quad n = 1,2,\ldots,N. \tag{57}$$

In the following, we present some numerical results on the macroscopic behavior of the

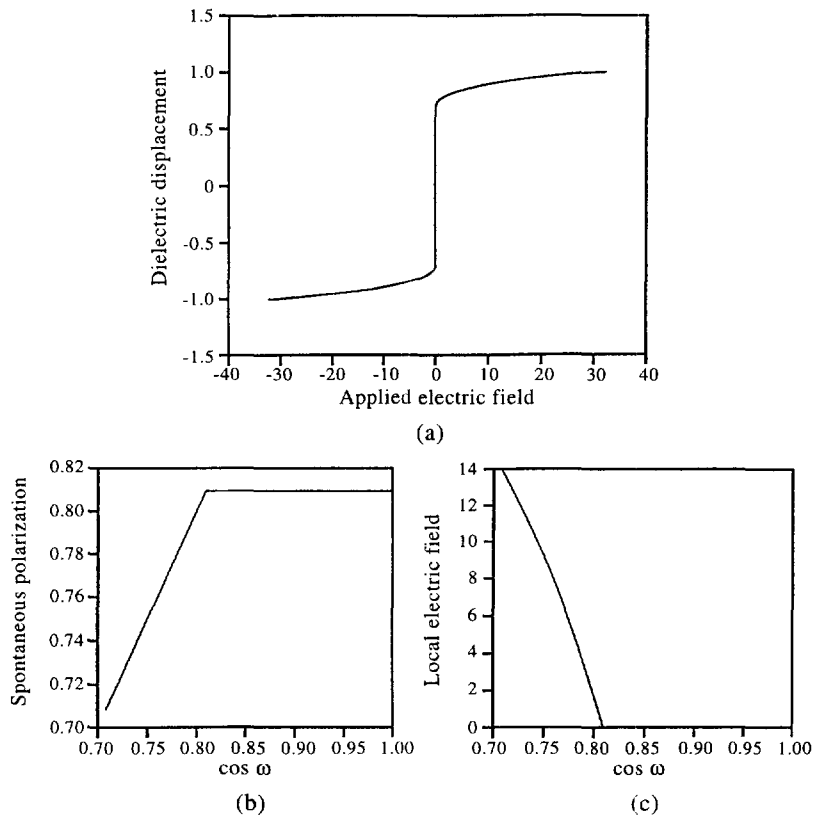

Fig. 1. The interior and saturated minimizers; (a) the dielectric displacement (d) response to the applied electric field (e_a); (b) variation of the crystallite spontaneous polarization (p^s) with the crystallite orientation angle (ω); (c) dependence of the local electric field (e) within the crystallites upon the orientation angle.

idealized specimen described above. We consider 500 crystallites, i.e., $N = 500$. For comparison, we first consider a case that only the minimizers are accessible and the corresponding results are shown in Fig. 1. As discussed in Section 3, the dielectric displacement d should be within the range: $-p^s \cos\omega_1 \leqslant d \leqslant p^s \cos\omega_1$, in the absence of applied electric field, i.e., $e_a = 0$. This corresponds to the vertical straight line segment in Fig. 1(a). For a positive e_a, one can find an integer k satisfying the inequalities in (46), indicating that the first k crystallites are saturated. The similar conclusion can be drawn for a negative e_a, as discussed in Section 3. The two curved segments in Fig. 1(a) correspond, respectively, to the ranges: $0 < e_a \leqslant 2e_c$ and $-2e_c \leqslant e_a < 0$. The spontaneous polarization of each crystallite corresponding to $e_a = 2e_c$ is plotted, in Fig. 1(b), vs the cosine of its orientation angle ω. The horizontal straight line segment indicates that crystallites with smaller orientation angle ω are saturated, and hence the local electric field within these crystallites vanishes, as shown in Fig. 1(c). Note that both the polarization p and the dielectric displacement d are normalized by the spontaneous polarization magnitude p^s, and that the electric field e is normalized by the coercive field e_c.

We now consider a quasi-static process with domain switching in response to an alternating electric field: $e_a(t) = 2e_c \sin t$. We used the mass fractions z_z^n given in (55) for the initial configuration and consequently, the specimen had no macroscopic polarization initially. Thus, the dielectric displacement response to the applied electric field, plotted in Fig. 2(a), is initiated from the origin. The dielectric displacement increases very slowly at the beginning until the applied electric field gets sufficiently strong to switch the domains according to the local switching criterion (48), and it then increases sharply due to massive domain switching, as shown in Fig. 2(a). As the applied electric field further increases to reach its maximum, the dielectric displacement arguments slowly and remains nonlinear due to continuous domain switching, at a much slower rate. The dielectric displacement

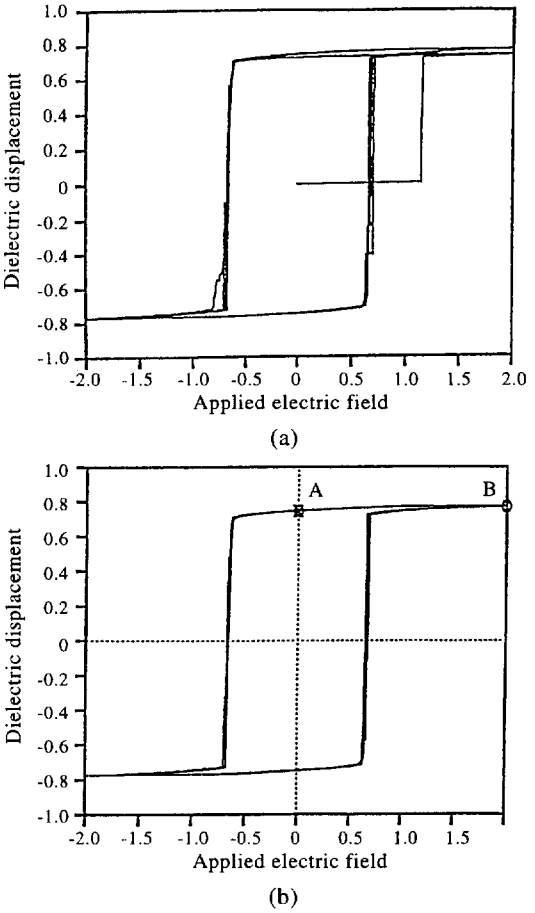

Fig. 2. Hysteretic behavior in the dielectric displacement response to the applied electric field; (a) the first five cycles; (b) the sixteenth to twentieth cycles.

response to the applied electric field is plotted in Fig. 2(a) for the first five cycles of the alternating field. The macroscopic response exhibits hysteresis, as expected. The discrepancy among different cycles is due to the influence of the initial condition. The macroscopic response repeats very well during the later cycles, and it is shown in Fig. 2(b) for the five consecutive cycles beginning with the sixteenth. After being subjected to an alternating electric field of magnitude large enough to induce domain switching, the specimen remains polarized even in the absence of applied electric fields. Correspondingly, the local electric field may not vanish although its average e_a is zero, due to the misalignment of the crystallites. To illustrate this point, we consider a state of spontaneous polarization that corresponds to the point marked with letter A in Fig. 2(b) and we plot, in Fig. 3(a), the electric field within each of the crystallites vs the cosine of its orientation angle ω. Correspondingly, the spontaneous polarization for each of the crystallites is shown in Fig. 3(b). Corresponding to the point marked with letter B in Fig. 2(b) where the applied electric field reaches its maximum $2e_c$, the electric field and the spontaneous polarization for every crystallite are plotted, respectively, in Figs 4(a) and (b), vs the cosine of its orientation angle ω. At this point, the local electric field is close to zero within those crystallites oriented close to the x axis (with a small ω), indicating that these crystallites are nearly saturated. Consequently, the rest of the crystallites are subjected to a local electric field of magnitude substantially larger than that of the applied electric field. This suggests that misalignment of crystallites can cause strong electric field concentration. In a real ferroelectric system, electric field concentration is usually linked with stress concentration due to the strong electromechanical coupling effect (Zhang and Jiang, 1995). We are unable to explore this issue with the present example because of the limitation of the one-dimensional setting. An attempt to analyze an electro-mechanically coupled example in higher dimensions would

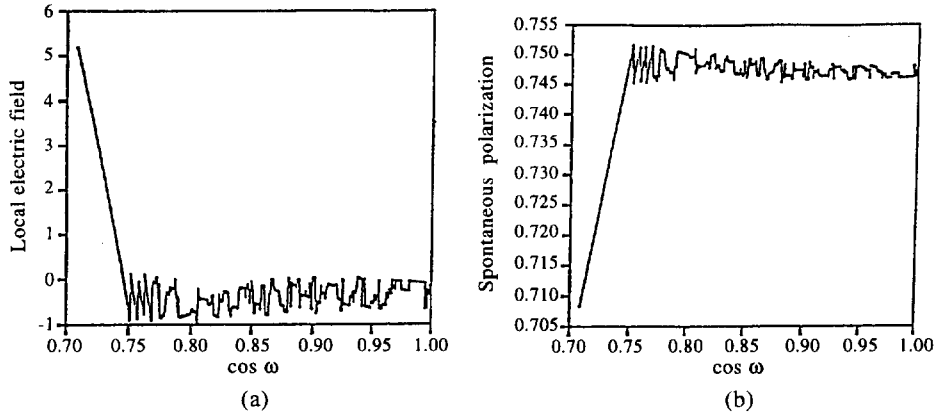

Fig. 3. A state of spontaneous polarization; (a) non-vanishing local electric field within crystallites in the absence of applied electric fields, due to crystallite orientation mismatch; (b) variation of crystallite spontaneous polarization due to orientation mismatch.

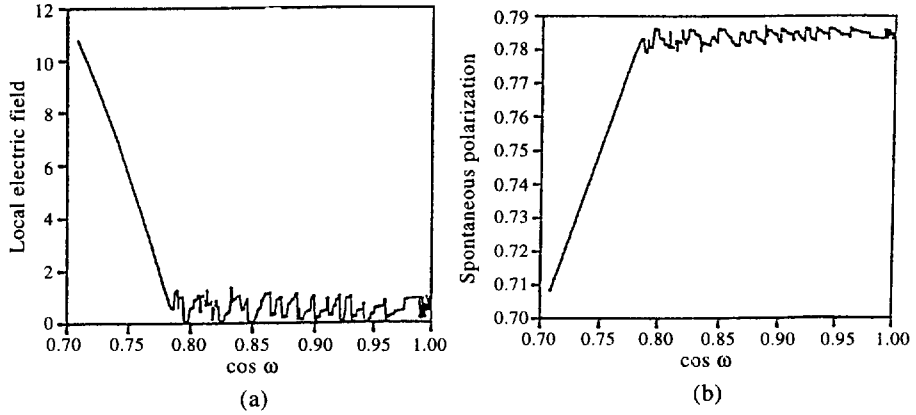

Fig. 4. A polarized state under an applied electric field; (a) local electric field concentration due to crystallite orientation mismatch; (b) variation of crystallite spontaneous polarization due to orientation mismatch.

necessarily involve a large amount of computational work. We are currently implementing this model with a numerical scheme in order to simulate the experiments with more realistic systems.

Acknowledgement—This work was supported by the Solid Mechanics Program at the US Office of Naval Research through Grant No. N00014-94-1-0053, and by the Mechanics and Materials Program at the National Science Foundation through Grant No. MSS-9308341.

REFERENCES

Abeyaratne, R. (1980) Discontinuous deformation gradients in plane finite elastostatics of incompressible materials. *Journal of Elasticity* **10**, 255–293.

Abeyaratne, R. and Knowles, J. K. (1988) On the dissipative response due to discontinuous strains in bars of unstable elastic material. *International Journal of Solids and Structures* **24**, 1021–1044.

Ball, J. and James, R. D. (1987) Fine phase mixtures as minimizers of energy. *Archive for Rational Mechanics and Analysis* **100**, 13–52.

Cao, H. and Evans, A. G. (1994) Electric-field-induced fatigue crack growth in piezoelectrics. *Journal of American Ceramic Society* **77**, 1783–1786.

Carl, K. (1975) Ferroelectric properties and fatiguing effects of modified $PbTiO_3$ ceramics. *Ferroelectrics* **9**, 23–32.

Crawley, E. F. and de Luis, J. (1987) Use of piezoelectric actuators as elements of intelligent structures. *AIAA Journal* **5**, 1373–1385.

Cross, L. E., (1993) Ferroelectric ceramics: tailoring properties for specific applications. In *Ferroelectric Ceramics*, eds Setter, N. and Colla, E. L., pp. 1–86. Birkhäuser Verlag, Basel.

Cross, L. E. (1994) Materials for adaptive structural acoustic controls. Technical Report, Office of Naval Research Contract No. N00014-92-J-1510, Office of Naval Research, UK.

Ericksen, J. L. (1975) Equilibrium of bars. *Journal of Elasticity* **5**, 191–201.

Freiman, S. W. and White, G. S. (1995) Intelligent ceramic materials : issues of brittle fracture. *Journal of Intelligent Material Systems and Structures* **6,** 49–54.

Giurgiutiu, V., Chaudhry, Z. and Rogers, C. A. (1994) Engineering feasibility of induced strain actuators for rotor blade active vibration control. In *Proceedings of the* 1994 *SPIE Smart Structures and Materials Conference*, ed. Hagood, N. W. SPIE Publications, Bellingham.

Hill, M. D., White, G. S., Hwang, C. S. and Lloyd, I. (1996) Cyclic damage in PZT. *Journal of American Ceramic Society* **79,** 1915–1920.

Huo, Y. and Jiang, Q. (1996) Modeling of domain switching in polycrystalline ferroelectric ceramics. *Smart Materials & Structures*, in press.

Jaffe, B., Cook, W. R. and Jaffe, H. (1971) *Piezoelectric Ceramics*. Academic Press, New York.

James, R. D. (1981) Finite deformation by mechanical twinning. *Archive for Rational Mechanics and Analysis* **77,** 143–176.

James, R. D. and Kinderlehere, D. (1993) Theory of magnetostriction with application to $Tb_xD_{y1-x}Fe_2$. *Philosophical Magazine* **B68,** 237–274.

Jiang, Q. (1993) Macroscopic behavior of a bar undergoing the paralectric-ferroelectric phase transformation. *Journal of the Mechanics and Physics of Solids* **41,** 1599–1635.

Jiang, Q. (1994) On the mechanisms of microcracking in ferroelectric ceramics. In *Proceedings of the Second International Conference on Intelligent Materials*, eds Rogers, C. A. and Wallace, G. G. Technomic Publishing Co., Lancaster.

Jiang, Q. Y., Cao, W. and Cross, L. E. (1994) Electric fatigue in lead zirconate titanate ceramics. *Journal of the American Ceramic Society* **77,** 211–215.

Jiang, Q. Y. and Cross, L. E. (1993) Effect of porosity on electric fatigue behavior in PLZT and PZT ceramics. *Journal of Material Science* **28,** 4536–4543.

Jona, F. and Shirane, G. (1962) *Ferroelectric Crystals*. Pergamon Press, New York.

Kim, S. and Jiang, Q. (1996) Microcracking and electric fatigue of polycrystalline ferroelectric ceramics. *Smart Materials and Structures* **5,** 321–326.

Kim, J., Varadan, V. V. and Varadan, V. K. (1996) Finite element modeling of active noise control with optimal placement of multiple actuators. In *Mathematics and Control in Smart Structures*, eds Varadan, V. V. and Chandra, J. SPIE Publications, Bellingham.

Knowles, J. K. and Sternberg, E. (1975) On the ellipticity of the equations of nonlinear elastostatics for a special material. *Journal of Elasticity* **5,** 341–361.

Lynch, C. S. (1996) Residual stress contribution to fracture of ferroelectric ceramics. In *Mathematics and control in Smart Structures*, eds Varadan, V. V. and Chandra, J. SPIE Publications, Bellingham.

Park, S. and Sun, C. T. (1995) Fracture criteria for piezoelectric ceramics. *Journal of American Ceramic Society* **78,** 1475–1480.

Salaneck, W. R. (1972) Some fatiguing effects in 8/65/35 PLZT fine grained ferroelectric ceramics. *Ferroelectrics* **9,** 97–101.

Samak, D. K. and Chopra, I. (1993) A feasibility study to build a smart rotor : trailing edge flap actuation. In *Proceedings of the* 1993 *North American Conference on Smart Structures and Materials*, ed. Varadan, V. K. SPIE Publications, Bellingham.

Samak, D. K. and Chopra, I. (1994) Design of high force, high displacement actuators for helicopter rotors. In *Proceedings of the* 1994 *North American Conference on Smart Structures and Materials*, ed. Hagood, N. W. SPIE Publications, Bellingham.

Suo, Z., Kuo, M., Barnett, D. M. and Willis, J. R. (1992) Fracture mechanics for piezoelectric ceramics. *Journal of the Mechanics and Physics of Solids* **40,** 739–765.

Tsai, H. Y. and Rosakis, P. (1995) Dynamic Twinning Processes in Crystals. *International Journal of Solids and Structures* **32,** 2711–2723.

White, G. S., Hill, M. D., Hwang, C. S. and Freiman, S. W. (1995) Mechanical behavior of cyclically loaded PZT. *Journal of the American Ceramic Society*, in press.

Zhang, Y. and Jiang, Q. (1995) Twinning-induced stress and electric field concentrations in ferroelectric ceramics. *Journal of the American Ceramic Society* **78,** 3290–3296.